A Novel SFBC-OFDM Scheme for Doubly-Selective Channels

Sili Lu, *Student Member, IEEE*, Balachander Narasimhan, *Student Member, IEEE*
and Naofal Al-Dhahir, *Fellow, IEEE*

***Abstract*— Effective Inter-carrier Interference (ICI) mitigation for MIMO-OFDM requires accurate channel estimation which is very challenging due to the large number and fast time-varying nature of the channel parameters to be estimated using scattered pilots. We present a novel SFBC-OFDM scheme for doubly-selective channels and a reduced-complexity channel estimation algorithm which exploits the banded and sparse structure of the channel in the frequency and time-domains, respectively. Furthermore, we design an FIR-MMSE ICI cancellation algorithm for mobile SFBC-OFDM and demonstrate its effectiveness for Digital Video Broadcasting-Handheld (DVB-H) systems.**

***Index Terms*— OFDM, SFBC, ICI, Doppler effect, Alamouti scheme**

I. Introduction

Orthogonal Frequency Division Multiplexing (OFDM) is very sensitive to the channel time-selectivity which manifests itself as variations in the channel impulse response (CIR) within each OFDM symbol. This so-called Doppler effect results in ICI whose energy is proportional to the Doppler frequency due to receiver mobility and is a significant performance-limiting impairment for OFDM systems.

In most previous studies, a quasi-static channel is assumed where the CIR is assumed constant over each OFDM symbol and a conventional one-tap per subcarrier frequency-domain equalizer (FEQ) is used, which becomes highly suboptimal under high Doppler. In [1], we proposed a finite-impulse-response minimum-mean-square-error (FIR-MMSE) FEQ with few (typically 3) taps per subcarrier which utilizes the approximately banded structure of the channel matrix in the frequency-domain.

OFDM in a multiple-input multiple-output (MIMO) system, known as MIMO-OFDM, is an attractive transmission scheme for high-rate reliable broadband wireless communication. A prime example is the Alamouti space-time block code (STBC) [2] which can be integrated with OFDM systems to achieve spatial and multipath diversity gains and reduce the error floor due to ICI. However, under high mobility, implementing the Alamouti STBC over adjacent OFDM symbols is not effective due to the significant channel time variations [3]. Instead, space-frequency block coding (SFBC) was considered in [4] [5] where the Alamouti scheme is implemented over adjacent subcarriers within the same OFDM symbol and where the channel frequency response (CFR) is approximately constant[1]. However, the Alamouti structure is destroyed in the presence of ICI and the corresponding diversity gains are diminished. An ICI mitigation scheme for SFBC-OFDM based on multi-stage non-linear iterative interference cancellation was proposed in [6], however, it involves high complexity of implementation. In this paper, we design a novel *embedded* Alamouti SFBC-OFDM scheme and show how to efficiently integrate it with the low-complexity FIR-MMSE FEQ in [1]. To compute the MIMO FIR-MMSE FEQ coefficients, we investigate a reduced-complexity hybrid time/frequency-domain channel estimation algorithm to estimate the Q main diagonals of the frequency-domain channel matrix. Simulation results show that our proposed scheme can effectively combat ICI under high-mobility conditions.

This paper is organized as follows. In Section II, the OFDM system model is described and the FIR-MMSE FEQ design for the single-antenna case is briefly discussed. In Section III-A this design is generalized to the MIMO case and integrated with our new embedded SFBC-OFDM system. A reduced-complexity channel estimation algorithm to estimate the fast-varying channel is described in Section IV and a detailed complexity analysis is given in Section IV-A. Simulation results are presented in Section V, and finally conclusions are drawn in Section VI.

Notation: We use $(\cdot)^T$ to denote the transpose, $(\cdot)^*$ the complex-conjugate, $\lfloor\cdot\rfloor$ the floor operation and $(\cdot)_N$ the modulo-N operation. $G_{i,j}$ denotes the element in the i-th row and j-th column of matrix $\mathbf{G}$. The estimated value of a random variable a is denoted by $\hat{a}$. $\mathbf{I}_N$ denotes the $N \times N$ identity matrix and $\mathbf{G}(:, j)$ denotes the j-th column of $\mathbf{G}$.

II. System Model and Assumptions

A. Mobile OFDM

Consider an OFDM system with N subcarriers where each OFDM symbol, denoted by $\mathbf{X} = [X_0 \dots X_{N-1}]^T$, is converted into time-domain samples $\mathbf{x} = [x_0 \dots x_{N-1}]^T$ using the N-point Inverse Fast Fourier Transform (IFFT) operation $\mathbf{x} = \mathbf{F}^H\mathbf{X}$ where $\mathbf{F}^H$ is the N-point IFFT matrix. The cyclic prefix (CP) length is assumed to be equal to or larger than the Channel Impulse Response (CIR) memory length denoted by ν. Hence, the received OFDM symbol $\mathbf{y} = [y_0 \dots y_{N-1}]^T$ after CP removal is given by

$$\mathbf{y} = \mathbf{H}\mathbf{x} + \mathbf{v} \tag{1}$$

This work was supported in part by Semiconductor Research Corporation under contract No. 2005-HJ-1328 and by a gift from Texas Instruments Inc.

The authors are with the University of Texas at Dallas, Email: {sxl059000,bxn062000,aldhahir}@utdallas.edu

[1]This will be the case when the FFT size is chosen large enough such that the channel coherence bandwidth is much larger than the subcarrier width, as in the DVB systems.

where $\mathbf{H}$ is an $N \times N$ time-domain channel matrix with elements $H_{n,l} = h_{n,(n-l)_N}$ where $h_{n,l}$ is the CIR at lag l for $0 \leq l \leq \nu - 1$ and time instant n for $0 \leq n \leq N-1$, and $\mathbf{v}$ is the time-domain noise vector with correlation matrix $\sigma^2\mathbf{I}_N$. Applying the FFT to (1), we obtain

$$\mathbf{Y} = \mathbf{F}\mathbf{y} = \mathbf{F}\mathbf{H}\mathbf{F}^H\mathbf{X} + \mathbf{F}\mathbf{v} = \mathbf{G}\mathbf{X} + \mathbf{V} \tag{2}$$

where $\mathbf{G} \triangleq \mathbf{F}\mathbf{H}\mathbf{F}^H$ is the frequency-domain channel matrix and $\mathbf{V}$ is the frequency-domain noise vector. For a quasi-static fading channel, $\mathbf{H}$ is a circulant matrix and hence transforms into a diagonal $\mathbf{G}$ matrix in (2). This in-turn decouples the sub-carriers, and a one-tap FEQ is optimal. However, for the time-varying channel, $\mathbf{H}$ is not circulant, and hence $\mathbf{G}$ is no longer diagonal. In this case, the input-output relation for the k-th subcarrier is given by

$$Y_k = G_{k,k}X_k + \sum_{n=0, n\neq k}^{N-1} G_{k,n}X_n + V_k \tag{3}$$

The first term on the right-hand side of (3) is the desired signal term while the second one is the ICI term which is characterized by the normalized Doppler frequency $F_d = f_dT$ where f_d is the Doppler frequency and T is the time duration of the data portion of one OFDM symbol.

For a MIMO system with M_r receive and M_t transmit antennas, we can generalize the model in (2) as follows. The frequency-domain channel matrix is $\mathbf{G} \in \mathbb{C}^{N.M_r \times N.M_t}$ whose (i,j)th block is the $N \times N$ frequency-domain channel matrix between the i-th receiver and j-th transmitter, denoted by $\mathbf{G}^{(i,j)} = \mathbf{F}\mathbf{H}^{(i,j)}\mathbf{F}^H$ and $\mathbf{H}^{(i,j)}$ is the corresponding time-domain channel matrix. The receive and transmit symbols are denoted by $\mathbf{Y} = [(\mathbf{Y}^{(1)})^T \ \ldots (\mathbf{Y}^{(M_r)})^T]^T \in \mathbb{C}^{N.M_r}$ and $\mathbf{X} = [(\mathbf{X}^{(1)})^T \ \ldots (\mathbf{X}^{(M_t)})^T]^T \in \mathbb{C}^{N.M_t}$ are the receive and transmit symbols, respectively, where $\mathbf{Y}^{(i)} = [Y_0^{(i)} \ \ldots \ Y_{N-1}^{(i)}]^T$ and $\mathbf{X}^{(j)} = [X_0^{(j)} \ \ldots \ X_{N-1}^{(j)}]^T$ for $1 \leq i \leq M_r$ and $1 \leq j \leq M_t$.

B. FIR-MMSE FEQ for SISO-OFDM

We approximate $\mathbf{G}$ by a banded matrix which has non-zero elements only along $(2D+1)$ main diagonals and two $D \times D$ triangular matrices in the top-right and bottom-left corners. Based on this banded structure, we proposed in [1] a reduced-complexity MMSE FEQ algorithm which computes for each subcarrier an FIR-MMSE FEQ based only on the following $(2D+1) \times (4D+1)$ submatrix of $\mathbf{G}$

$$\mathbf{G}_m = \begin{bmatrix} G_{(m-D)_N,(m-2D)_N} & \cdots & G_{(m-D)_N,(m+2D)_N} \\ \vdots & \vdots & \vdots \\ G_{m,(m-2D)_N} & \cdots & G_{m,(m+2D)_N} \\ \vdots & \vdots & \vdots \\ G_{(m+D)_N,(m-2D)_N} & \cdots & G_{(m+D)_N,(m+2D)_N} \end{bmatrix} \tag{4}$$

The Q-tap (where $Q = 2D+1$) FIR-MMSE FEQ is given by

$$\mathbf{w}_m = \mathbf{g}_m^H(\mathbf{G}_m\mathbf{G}_m^H + \sigma^2\mathbf{I}_Q)^{-1} \tag{5}$$

where $\mathbf{g}_m = \mathbf{G}_m(:, 2D+1)$ is the middle column of $\mathbf{G}_m$. Hence, the FIR-MMSE FEQ output for the m-th subcarrier is given by

$$\hat{X}_m = \mathbf{w}_m\mathbf{Y}_m \tag{6}$$

where $\mathbf{Y}_m = [Y_{(m-D)_N}, \ldots, Y_{(m+D)_N}]^T$.

This FIR-MMSE FEQ has $\mathcal{O}(NQ^2)$ complexity, compared to the conventional N-tap per subcarrier FEQ which has $\mathcal{O}(N^3)$ complexity. In [1], we showed that for a normalized Doppler spread of up to 10%, choosing a 3-tap FEQ (i.e. $Q = 2D+1 = 3$) achieves a favourable performance-complexity tradeoff.

III. FIR-MMSE FEQ for MIMO-OFDM

In this section, we generalize our FIR-MMSE FEQ design to the MIMO case and propose a new embedded Alamouti SFBC-OFDM scheme which can be readily integrated with the FIR-MMSE FEQ. Here, we consider pilot-symbol-assisted channel estimation where the pilot tones are embedded in each OFDM symbol.

A. Conventional SFBC-OFDM

In a conventional SFBC-OFDM system [5], pairs of information symbols (X_1, X_2) are fed to the SFBC encoder according to the Alamouti encoding rule [2]

$$\begin{bmatrix} X_1 \\ X_2 \end{bmatrix} \rightarrow \begin{bmatrix} X_1 & X_2 \\ -X_2^* & X_1^* \end{bmatrix} \begin{matrix} \rightarrow \\ \downarrow \end{matrix} \begin{matrix} \text{space} \\ \text{subcarrier} \end{matrix}$$

Hence, each Alamouti codeword spans two adjacent subcarriers. Assuming the CFR fixed over each pair of adjacent subcarriers, each orthogonal Alamouti codeword can be detected optimally using a space-frequency matched filter in the absence of ICI. However, in the presence of high Doppler, severe ICI from adjacent subcarriers destroys the Alamouti structure resulting in significant performance degradation, which motivates this work.

B. Embedded Alamouti SFBC-OFDM

We consider an Alamouti SFBC-OFDM system with $M_t = 2$ transmit and M_r receive antennas. The signal at the ith receive antenna is given by

$$\mathbf{Y}^{(i)} = \mathbf{G}^{(i,1)}\mathbf{X}^{(1)} + \mathbf{G}^{(i,2)}\mathbf{X}^{(2)} + \mathbf{V} \tag{7}$$

Similar to the SISO case in Section II-B, each $\mathbf{G}^{(i,j)}$ is approximately a banded matrix with $Q = (2D+1)$ non-zero diagonals. In order to guarantee spatial diversity gains (by preserving the Alamouti structure) in the presence of severe ICI and exploit the banded structure of $\mathbf{G}^{(i,j)}$, we design our SFBC encoding scheme as shown in Fig. 1. Each OFDM symbol of size N is divided into data blocks each consisting of L subcarriers separated by D pilot subcarriers where D is equal to the number of significant superdiagonals in $\mathbf{G}^{(i,j)}$. Two information symbols are grouped into pairs and form an Alamouti codeword which is implemented over the k-th ($1 \leq k \leq L$) subcarriers of two adjacent data blocks which are separated by $B = L + D$ subcarriers. As shown in Fig. 1, two adjacent data blocks and their two corresponding

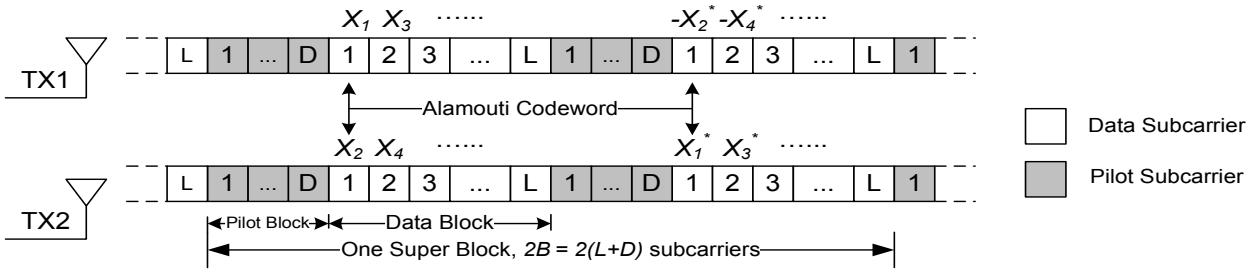

Fig. 1. Proposed embedded Alamouti SFBC-OFDM frame structure

pilot blocks form one *superblock*; hence, each superblock spans $2B$ subcarriers and contains L Alamouti codewords. For each non-edge codeword (i.e. $k \neq 1$ or L), ignoring noise and considering (for simplicity) ICI only from the adjacent subcarrier (i.e. $D = 1$) at the i-th receive antenna, we have

$$\begin{aligned}\mathbf{Y}_k^{(i)}(l) =& \mathbf{G}_{k,k-1}^{(i)}(l)\mathbf{X}_{k-1}(l) + \mathbf{G}_{k,k}^{(i)}(l)\mathbf{X}_k(l) \\ &+ \mathbf{G}_{k,k+1}^{(i)}(l)\mathbf{X}_{k+1}(l)\end{aligned} \tag{8}$$

where $\mathbf{Y}_k^{(i)}(l) = [Y_{2lB+k}^{(i)} \ (Y_{2lB+k+B}^{(i)})^*]^T$ and $\mathbf{X}_k(l) = [X_{2lB+2k-1} \ X_{2lB+2k}]^T$ correspond to the receive and transmit pair for the k-th Alamouti codeword in the l-th superblock, respectively, for $2 \leq k \leq L-1$. $\mathbf{G}_{k,m}^{(i)}(l)$ is the CFR for the k-th Alamouti codeword given by

$$\mathbf{G}_{k,m}^{(i)}(l) = \begin{bmatrix} G_{2lB+k,2lB+m}^{(i,1)} & G_{2lB+k,2lB+m}^{(i,2)} \\ (G_{2lB+k+B,2lB+m+B}^{(i,2)})^* & -(G_{2lB+k+B,2lB+m+B}^{(i,1)})^* \end{bmatrix} \tag{9}$$

It is clear that $\mathbf{G}_{k,k}^{(i)}(l)$ is at the main diagonal of $\mathbf{G}$; hence, the second term on the right-hand side of (8) is the desired term while the other two are ICI terms. Using this form, we can easily extend the SISO FIR-MMSE FEQ of Section II-B to the Alamouti SFBC case which will be discussed in the next subsection.

A key advantage of our proposed SFBC-OFDM scheme is that each Alamouti codeword experiences ICI only from its neighboring Alamouti codewords as shown in (8) while the ICI within each Alamouti codeword is negligible since the 2 subcarriers in each Alamouti codeword are separated by $B = L + D$ subcarriers.

We note that the first ($k = 1$) and last ($k = L$) Alamouti codewords of each superblock experience ICI from a non-Alamouti codeword on their left and right sides, respectively; hence, Equation (8) does not hold for these edge codewords. To mitigate the ICI for these edge codewords, we insert two pilot blocks, each composed of D subcarriers as shown in Fig. 1. Since the pilot subcarriers are known to the receiver, their interference to the edge codewords in each data block can be computed and cancelled from the received signal to facilitate equalization. This can be viewed as the dual of the role of the guard interval in the time-domain which cancels inter-symbol interference (ISI) between successive OFDM symbols.

We emphasize that this scheme is different from STBC-OFDM [2] in that the Alamouti scheme is implemented over the kth subcarriers of two adjacent OFDM symbols and is not suitable for the fast time-varying channel conditions considered in this paper. It is also different from conventional SFBC-OFDM [5], in that the Alamouti scheme is implemented over adjacent subcarriers and fails in the presence of severe ICI between adjacent subcarriers. In both of these schemes, the Alamouti structure is destroyed and hence spatial diversity gains can not be realized. Our proposed scheme solves this problem. To achieve full spatial diversity, $\mathbf{G}_{k,m}^{(i)}(l)$ must be as close to the Alamouti matrix as possible. This requires $G_{k,m}^{(i,j)} \approx G_{k+B,m+B}^{(i,j)}, j = 1, 2$, or equivalently, the channel coherence bandwidth must be much larger than the width of B subcarriers. For the TU06 channel model we use in this paper for the DVB environment[2], the channel coherence bandwidth is around 200 KHz while the subcarrier width is 1 KHz for the 8K mode. Hence, the CFR can be approximated as fixed over tens of subcarriers. For normalized Doppler up to 10%, we will sow in Section V that $D = 1$ represents good performance-complexity trade-off.

The choice of the design parameter L entails a rate-reliability trade-off. Choosing a larger L results in higher data-rate but less diversity gain (since the channel frequency response fluctuates more within each Alamouti codeword). On the other hand, a smaller L results in a lower data rate but approximating (9) as an Alamouti matrix becomes more accurate resulting in higher diversity gain.

C. FIR-MMSE FEQ for Embedded Alamouti SFBC-OFDM

In this section, we integrate the FIR-MMSE FEQ in Section II-B with our Alamouti SFBC-OFDM scheme in Section III-B. For the m-th Alamouti codeword of the l-th superblock, we omit the superblock index l, and construct a matrix $\mathbf{G}_m = [(\mathbf{G}_m^{(1)})^T \ \ldots \ (\mathbf{G}_m^{(M_r)})^T]^T$ as a stack of M_r matrices, each of which has a similar structure to (4) for the SISO case, i.e.

$$\mathbf{G}_m^{(i)} = \begin{bmatrix} \mathbf{G}_{(m-D)_N,(m-2D)_N}^{(i)} & \cdots & \mathbf{G}_{(m-D)_N,(m+2D)_N}^{(i)} \\ \vdots & \vdots & \vdots \\ \mathbf{G}_{m,(m-2D)_N}^{(i)} & \cdots & \mathbf{G}_{m,(m+2D)_N}^{(i)} \\ \vdots & \vdots & \vdots \\ \mathbf{G}_{(m+D)_N,(m-2D)_N}^{(i)} & \cdots & \mathbf{G}_{(m+D)_N,(m+2D)_N}^{(i)} \end{bmatrix} \tag{10}$$

[2]As discussed in [7], the accuracy of the TU06 channel model for the mobile DVB environment was verified experimentally

where each element of $\mathbf{G}_m^{(i)}$ is a 2×2 matrix of the form given in (9) (setting $l = 0$ to omit the superblock index). Hence, similar to (5), the FIR-MMSE FEQ coefficients are given by

$$\mathbf{w}_m = \mathbf{g}_m{}^H (\mathbf{G}_m \mathbf{G}_m{}^H + \sigma^2 \mathbf{I}_{2QM_r})^{-1} \tag{11}$$

where $\mathbf{g}_m \in \mathbb{C}^{2QM_r \times 2}$ contains the middle two columns of $\mathbf{G}_m$ and $\mathbf{w}_m \in \mathbb{C}^{2 \times 2QM_r}$ is the FIR-MMSE FEQ coefficient matrix. Finally, the FEQ output for the m-th codeword is $\hat{\mathbf{X}}_m = \mathbf{w}_m \mathbf{Y}_m$ where $\hat{\mathbf{X}}_m = [\hat{X}_{2m-1}\ \hat{X}_{2m}]^T$, $\mathbf{Y}_m = [(\bar{\mathbf{Y}}_m^{(1)})^T \ \dots (\bar{\mathbf{Y}}_m^{(M_r)})^T]^T$ and $\bar{\mathbf{Y}}_m^{(i)} = [Y_{(m-D)_N}^{(i)} \ (Y_{(m-D+B)_N}^{(i)})^* \ \dots \ Y_{(m+D)_N}^{(i)} \ (Y_{(m+D+B)_N}^{(i)})^*]^T$. We conclude this section by noting that our embedded SFBC-OFDM scheme can be directly extended to $M_t > 2$ transmit antennas using complex orthogonal designs [8]. However, the CFR must be fixed over $(M_t - 1)B = (M_t - 1)(L + \nu)$ subcarriers which reduces the allowable upper-bound on L. In addition, the complexity involved in computing and applying the FEQ weights increases.

IV. Simplified Hybrid Frequency/time Channel Estimation

We assumed a tri-diagonal ($D = 1$) banded structure for $\mathbf{G}$ in Fig. 1. Furthermore, we consider $P = \frac{N}{B}$ pilot subcarriers equally spaced at $X_{p(0)}, \cdots, X_{p(P)}$ where $p(l) = l \times B$ and each superblock contains one Alamouti pilot codeword, i.e. two pilot subcarriers separated by B subcarriers. Assuming the channels fixed over B adjacent subcarriers (i.e.$G_{k,k}^{(i,j)} \approx G_{k+B,k+B}^{(i,j)}, j = 1, 2$ and $1 \le i \le M_r$) and ignoring ICI and noise, we obtain the following input-output relation for subcarriers $p(l)$ and $p(l) + B$ for the i-th receive antenna

$$\begin{bmatrix} Y_{p(l)}^{(i)} \\ Y_{p(l)+B}^{(i)} \end{bmatrix} = \begin{bmatrix} X_{p(l)} & X_{p(l)+B} \\ -X_{p(l)+B}^* & X_{p(l)}^* \end{bmatrix} \begin{bmatrix} G_{p(l),p(l)}^{i,1} \\ G_{p(l),p(l)}^{i,2} \end{bmatrix} \tag{12}$$

which is used to obtain the least squares (LS) estimate for the CRF at the main diagonal of $\mathbf{G}^{(i,j)}$. To estimate the $Q = 3$ diagonals of $\mathbf{G}^{(i,j)}$ (i.e. the main diagonal and the first sub- and super-diagonals), we extend the hybrid frequency/time-domain channel estimation algorithm in [9] to the MIMO case. This algorithm exploits the fact that for normalized Doppler of up to 20%, the channel time-variations can be approximated by a piece-wise linear model with a constant slope over each OFDM symbol. We summarize the algorithm in [9] and extend it to the MIMO case as follows.

Step 1 Ignoring ICI, for each receive antenna i, we obtain the CFR at the pilot codeword locations using (12) and compute $\hat{G}_{p(l),p(l)}^{(i,j)}$ for $j = 1, 2$ and $1 \le i \le M_r$. For each transmit-receive antenna pair, we omit the i, j indices to simplify the notation, since we are estimating each of the $2M_r$ frequency-domain channel matrices *independently*. After linear or Wiener filtering interpolation on $\hat{G}_{p(l),p(l)}$, we obtain an estimate of the diagonal of $\mathbf{G}$, denoted by $\hat{\mathbf{g}}$, followed by a P-point IFFT to estimate the average CIR (i.e. the middle row of $\mathbf{H}$) denoted by $\mathbf{h}_{t-1}^{\text{avg}}$ where we assume that the current OFDM symbol index is $t - 1$.

Step 2 Repeat Step 1 for the next two OFDM symbols to calculate the middle rows for three consecutive OFDM symbols, denoted by $\hat{\mathbf{h}}_{t-1}^{\text{avg}}$, $\hat{\mathbf{h}}_t^{\text{avg}}$ and $\hat{\mathbf{h}}_{t+1}^{\text{avg}}$.

Step 3 For the current OFDM symbol, we denote by $\hat{\boldsymbol{\alpha}}_1$ and $\hat{\boldsymbol{\alpha}}_2$ the estimated slope vectors for the first and second halves of the OFDM symbol, respectively. Hence

$$\hat{\boldsymbol{\alpha}}_1 = (\hat{\mathbf{h}}_t^{\text{avg}} - \hat{\mathbf{h}}_{t-1}^{\text{avg}})/N; \hat{\boldsymbol{\alpha}}_2 = (\hat{\mathbf{h}}_{t+1}^{\text{avg}} - \hat{\mathbf{h}}_t^{\text{avg}})/N \tag{13}$$

Step 4 Using the CIR slope vectors, we calculate the estimated off-diagonal elements of $\mathbf{G}$ (see [10]). Combined with the estimated main diagonal obtained from Step 1, we now have an estimate of the full $\mathbf{G}$ matrix which we denote by $\hat{\mathbf{G}}$.

To further reduce the complexity of this hybrid channel estimation algorithm, we exploit the *sparseness* of the time-domain CIR and the *banded* structure of the frequency-domain channel matrix $\mathbf{G}$. In practice, the CIR in DVB applications is usually sparse and the number of active channel taps is much less than L. Hence, many channel taps can be zeroed out to reduce the processing complexity with negligible performance loss. To do this, we choose the M taps from $\hat{\mathbf{h}}^{\text{avg}}$ with the largest absolute value, and zero out all the remaining taps. Therefore, we only need to estimate M instead of L slopes when calculating $\hat{\boldsymbol{\alpha}}_1$ and $\hat{\boldsymbol{\alpha}}_2$ in (13). Choosing the value of M entails a complexity-performance tradeoff.

Further, we exploit the banded structure of $\mathbf{G}$ to reduce channel estimation complexity. Simulation results in Section V show that a 3-tap FEQ [1] which requires an estimate of only the three main diagonals of $\mathbf{G}$ performs well (and only within 0.5dB from a 5-tap FEQ) even at a relatively high normalized Doppler of 10% . Since the main diagonal of $\mathbf{G}$ is estimated in Step 1, we only need to compute one sub-diagonal and one super-diagonal of $\hat{\mathbf{G}}$ in Step 4 instead of the full matrix. Furthermore, we proved in [10] that the elements of the sub-diagonals are approximately the negatives of the corresponding elements of the super-diagonals for large N; hence, we only need to compute one super-diagonal of $\hat{\mathbf{G}}$.

A. Complexity Analysis

For the SISO case, Steps 1-3 have much lower complexity than Step 4 in Section IV. In Step 4, a closed-form expression to compute the off-diagonal elements of $\mathbf{G}$ from $\hat{\boldsymbol{\alpha}}_1$ and $\hat{\boldsymbol{\alpha}}_2$ was given in [10]. We first need to calculate two N-point IFFT of an L-sample vector [3] (namely $\hat{\boldsymbol{\alpha}}_1 + \hat{\boldsymbol{\alpha}}_2$ and $\hat{\boldsymbol{\alpha}}_1 - \hat{\boldsymbol{\alpha}}_2$), which has a complexity of $[\log_2 L + 2(1 - \frac{L}{N})] \cdot \frac{N}{2}$ complex multiplications each [11]. In [12], a generic FFT pruning algorithm is proposed which does not require the sparse input data to be grouped together (as in our case where the M active CIR taps are dispersed among the entire L CIR taps). This algorithm has a complexity saving ratio of β, which is defined as the ratio of number of complex multiplications saved using this algorithm (see [12]) and the number of complex multiplications required to perform one set of conventional FFT operation; Hence, we need approximately $(1 - \beta)[\log_2 L + 2(1 - \frac{L}{N})]N$ complex multiplications for

[3]These L samples are grouped together.

TABLE I

COMPLEXITY FOR HYBRID CHANNEL ESTIMATION ALGORITHM

	# of multiplications ($N_{multi.}$)		
System	single antenna	2-TX 1-RX	2-TX 2-RX
M=10, D=1	13850	27700	55400
M=10, D=2	15898	31796	63592
M=10, D=N-1	6.2×10^6	1.2×10^7	2.4×10^7
M=64, D=1	20253	40506	81012
M=64, D=2	22400	44800	89600
M=64, D=N-1 (as in [9])	6.2×10^6	1.2×10^7	2.4×10^8

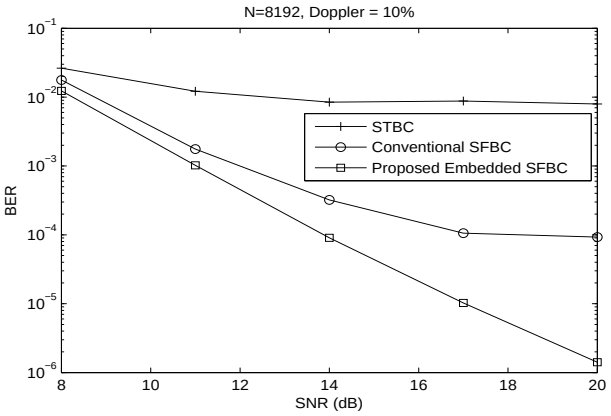

Fig. 2. BER comparison for STBC, conventional SFBC and our proposed embedded SFBC with perfect channel and 10% Doppler

2 IFFT operations, where β is given in [12] for different scenarios. Furthermore, to compute 1 off-diagonal element of $\hat{\mathbf{G}}$, we need 2 complex multiplications for odd-indexed diagonals and 1 for even-indexed diagonals [10]. We estimate D subdiagonals for a Q-tap FEQ (where $Q = 2D+1$), which requires $(3\lfloor\frac{D}{2}\rfloor + 2(D)_2)N$ complex multiplications (see [10] for details). Denoting the total number of multiplications by $N_{multi.}$, we have

$$N_{multi.} = (1-\beta)(\log_2 L + 2(1-\frac{L}{N}))N + (3\lfloor\frac{D}{2}\rfloor + 2(D)_2)N \quad (14)$$

For the MIMO case, we repeat the same procedure for all $M_t \times M_r$ channels; hence the complexity will increase linearly by a factor of $M_t \times M_r$. Table I lists the total number of multiplications used by the hybrid channel estimation algorithm assuming a CIR with $L = 64$ taps and $N = 2048$ for different M and D. By using $M = 10$ instead of 64 as is the case for the conventional scheme in [9], the IFFT complexity is reduced by approximately 40% (i.e. $\beta \approx 0.4$) [12]. In addition, by exploiting the banded structure of $\mathbf{G}$ (i.e. assuming a tri-diagonal $\mathbf{G}$ with $D = 1$ instead of a full $\mathbf{G}$ with $D = N - 1$ as is the case for the scheme in [9]), the number of required multiplies is reduced significantly.

V. SIMULATION RESULTS

We consider the DVB-H standard as our case study, which supports high mobility. We focus on the 8K mode of DVB-H with $N = 8192$ subcarriers since it suffers more from ICI than the 2K or 4K modes. We adopt the typical urban TU-06 channel delay profile defined by the COST 207 project with 6 taps

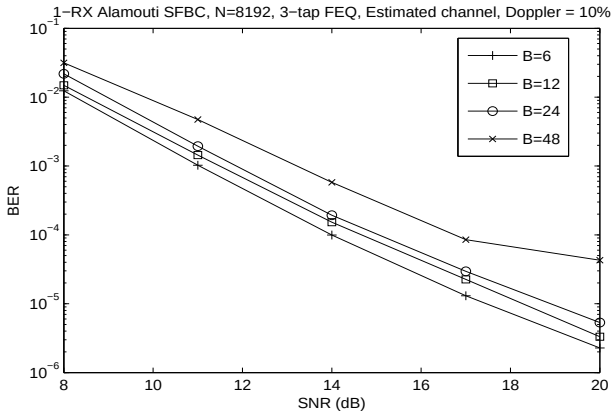

Fig. 3. 1-RX embedded Alamouti SFBC-OFDM with different B and 10% Doppler

in the continuous-time domain, 8 MHz channel bandwidth, and a carrier frequency of 800 MHz. After sampling, a discrete-time CIR with approximately 50 taps is obtained. Each discrete channel tap is generated by an independent complex Gaussian random variable with time correlation based on Jakes' model. Furthermore, we use a 64-state rate-1/2 convolutional code and the coded bits are interleaved and mapped into QPSK constellation points.

The BER performance for the 8K mode system is evaluated at a relatively high normalized Doppler of 10% corresponding to a highway speed of approximately 130 Km/h in this simulation. We first compare our proposed embedded Alamouti SFBC scheme with the Alamouti STBC and the conventional SFBC scheme assuming perfect channel knowledge at the receiver. Fig. 2 shows that the Alamouti STBC fails in the presence of high Doppler, since the channel is fast time-varying and the fixed channel assumption for the Alamouti codeword does not hold in this case. We also observe an error floor for the conventional SFBC with a 3-tap FEQ. This is due to the fact that conventional SFBC implements the Alamouti codeword over two adjacent subcarriers; hence, there will be ICI within each Alamouti codeword which destroys its orthogonality. Our proposed scheme eliminates the error floor by implementing the Alamouti codeword over non-adjacent subcarriers ($B = 12$ in this case) and integrating it with a 3-tap FEQ to further mitigate the ICI.

Fig. 3 shows the BER performance for a two-transmit and one-receive antenna system implementing our proposed embedded Alamouti SFBC scheme with different B. We observe that as B increases, the BER performance becomes worse (since the assumption of the Alamouti matrix structure in (9) becomes less accurate and due to the increased difficulty in channel interpolation between pilot subcarriers), but the pilot overhead is reduced.

Keeping the same 1/12 pilot overhead rate of the DVB standard, we insert a pilot for every 12 subcarriers ($B = 12$) and Fig. 4 shows the performance for this scenario. Since there is significant ICI, error floors are observed with a 1-tap FEQ with either perfect or estimated channel conditions. To combat this ICI, we implemented our 3-tap FEQ design as described

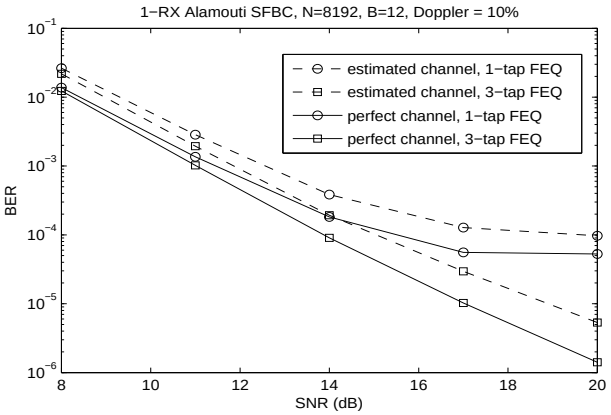

Fig. 4. 1-RX embedded Alamouti SFBC-OFDM and 10% Doppler

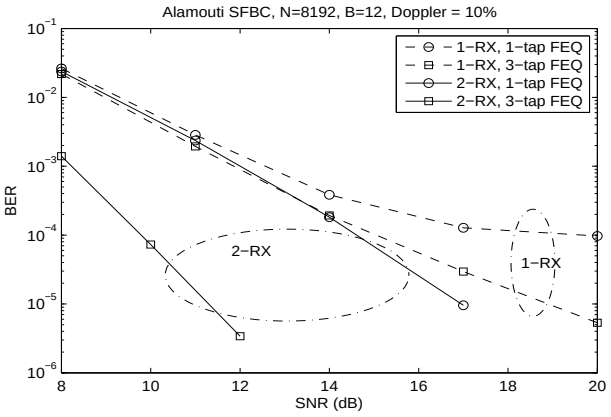

Fig. 5. Embedded Alamouti SFBC-OFDM with estimated channel and 10% Doppler

in Section III-A which improves performance significantly. To estimate the 3 main diagonals of $\mathbf{G}$, we implemented the reduced-complexity hybrid channel estimation algorithm in Section IV and it results in only 2 dB performance loss from the case of perfect channel knowledge.

Finally, to realize additional spatial diversity gains, we increased the number of receive antennas to 2. Fig. 5 compares the performances of the 1-RX and 2-RX systems (with estimated channel information) where the increased slope of the BER curves for the 2-RX case is evident and results in additional ICI mitigation.

VI. Conclusion

High mobility causes performance-limiting ICI in MIMO-OFDM receivers. We designed a novel SFBC-OFDM scheme and showed how to integrate it with FIR ICI-mitigating equalization. To compute the equalizer coefficients, we showed how to estimate the fast time-varying MIMO channel matrix efficiently by exploiting its sparse and banded structure in the time and frequency-domains, respectively. Simulation results for the DVB-H system demonstrate the effectiveness of our proposed scheme.

References

[1] S. Lu, R. Kalbasi, and N. Al-Dhahir, "OFDM interference mitigation algorithms for doubly-selective channels," *In Proc. of IEEE Vehicular Technology Conference*, pp. 1–5, Sep 2006.

[2] S. M. Alamouti, "A simple transmit diversity technique for wireless communications," *IEEE J. Select. Areas Commun.*, vol. 16, pp. 1451–1458, Oct 1998.

[3] J. Wu and G. J. Saulnier, "Orthogonal space-time block code over time-varying flat-fading channels: Channel estimation, detection, and performance analysis," *IEEE Trans. Commun.*, vol. 55, pp. 1077–1087, May 2007.

[4] M. Torabi, S. Aissa, and M. Soleymani, "On the BER performance of space-frequency block coded OFDM systems in fading MIMO channels," *IEEE Trans. Wireless Commun.*, vol. 6, pp. 1366–1373, Apr 2007.

[5] K. F. Lee and D. B. Williams, "A space-frequency transmitter diversity technique for OFDM systems," in *Proc. of IEEE Global Telecommunication Conference*, vol. 3, Nov 2000, pp. 1473–1477.

[6] D. Sreedhar and A. Chochalingam, "Detection of SFBC-OFDM signals in frequency and time-selective MIMO channels," in *Proc. of IEEE WCNC*, Mar 2007, pp. 852–857.

[7] S. Tomasin, A. Gorokhov, H. Yang, and J. Linnartz, "Iterative interference cancellation and channel estimation for mobile OFDM," *IEEE Trans. Wireless Commun.*, vol. 4, pp. 238–245, Jan 2005.

[8] V. Tarokh, H. Jafarkhani, and A. R. Calderbank, "Space-time block codes from orthogonal designs," *IEEE Trans. Inform. Theory*, vol. 45, pp. 1456–1467, Jul 1999.

[9] Y. Mostofi and D. Cox, "ICI mitigation for pilot-aided OFDM mobile systems," *IEEE Trans. Wireless Commun.*, vol. 4, pp. 765–774, Mar 2005.

[10] S. Lu and N. Al-Dhahir, "Reduced-complexity hybrid time/frequency channel estimation for DVB-H," in *Proc. of IEEE Sarnoff Symposium*, May 2007, Available at http://www.utdallas.edu/∼aldhahir/sarnoff_hest.pdf.

[11] J. Markel, "FFT pruning," *IEEE Trans. Audio Electroacoust.*, vol. 19, pp. 305–311, Dec 1971.

[12] Z. Hu and H. Wan, "A novel generic fast Fourier transform pruning technique and complexity analysis," *IEEE Trans. Signal Processing*, vol. 53, pp. 274–282, Jan 2005.